

Development of a novel electrochemical method for the quantitative analysis of vandetanib in the presence of anionic surfactant utilizing a bare carbon paste electrode

Pınar TALAY PINAR ^{1*} , Cihat METE ² , Zühre ŞENTÜRK ³ 

¹ Department of Analytical Chemistry, Faculty of Pharmacy, Van Yuzuncu Yil University, Van, Türkiye.

² Department of Pharmaceutical Chemistry, Faculty of Pharmacy, Van Yuzuncu Yil University, Van, Türkiye.

³ Department of Analytical Chemistry, Faculty of Science, Van Yuzuncu Yil University, Van, Türkiye.

* Corresponding Author. E-mail: ptalay@gmail.com (P.T.P.); Tel. +90-432-225 17 01.

Received: 5 April 2024 / Revised: 18 May 2024 / Accepted: 18 May 2024

ABSTRACT: In this investigation, a novel electrochemical approach employing a bare carbon paste electrode (CPE) has been devised for the sensitive and expeditious quantification of the tyrosine kinase inhibitor vandetanib (VAN). VAN, a pivotal anti-tumor agent employed in various cancer types, notably medullary thyroid cancer, manifested an irreversible oxidation peak at approximately +1.17 V (vs. Ag/AgCl, 3 M NaCl) in 0.1 M HNO₃, elucidated through cyclic voltammetry. The electrode reaction was determined to proceed via controlled adsorption. The study meticulously examined the influence of anionic surfactant sodium dodecyl sulfate (SDS), instrumental parameters, pH fluctuations, and the composition of the supporting electrolyte on the oxidation peak of VAN. Remarkably, the sensitivity of stripping voltammetric measurements markedly augmented upon the inclusion of 9×10^{-4} M SDS. Employing optimized parameters for SW-AdSV (square-wave adsorptive stripping voltammetry), the bare CPE demonstrated exceptional linearity within the dynamic ranges of 1.05×10^{-7} – 1.6×10^{-5} M for VAN. The limit of detection and limit of quantification were established at 2.7×10^{-8} and 9.0×10^{-8} M for VAN, respectively. Furthermore, the developed electrochemical methodology was effectively applied for the detection of VAN in spiked model serum samples.

KEYWORDS: Vandetanib; tyrosine kinase inhibitor; sodium dodecylsulfate; carbon paste electrode; biological sample.

1. INTRODUCTION

The effectiveness of targeted therapies represents a significant advancement in cancer treatment, particularly following chemotherapy. This efficacy has been demonstrated across various cancer types, including thyroid cancers, which have shown notable responses to targeted therapies comparable to colon, breast, and lung cancers, as well as neuroendocrine tumors, certain sarcomas, lymphomas, kidney cancers, and liver cancers. Targeted therapies encompass both large molecule drugs, such as monoclonal antibodies, and small molecule drugs that inhibit tyrosine kinase enzymes, thereby impeding cell growth, proliferation, and angiogenesis signaling pathways [1,3]. VAN (Figure 1) is among the tyrosine kinase inhibitors currently approved by the American Food and Drug Administration (US FDA) for the treatment of progressive, locally advanced, or metastatic medullary thyroid carcinomas (MTCs). It is an orally administered antiangiogenic tyrosine kinase inhibitor. VAN can be utilized either as monotherapy or in combination with other anticancer agents, including chemotherapy and radiotherapy, to devise comprehensive treatment regimens for various tumor types [4,7]. Chemically, Vandetanib (VAN) is described as N-(4-bromo-2-fluorophenyl)-6-methoxy-7-[(1-methylpiperidin-4-yl) methoxy] quinazolin-4-amine. It functions as a dual inhibitor targeting vascular endothelial growth factor receptor (VEGFR) and epidermal growth factor receptor (EGFR) tyrosine kinases, thereby disrupting critical pathways involved in tumor angiogenesis and growth [8-9].

How to cite this article: Talay Pınar P, Mete C, Şentürk Z. Development of a novel electrochemical method for the quantitative analysis of vandetanib in the presence of anionic surfactant utilizing a bare carbon paste electrode. J Res Pharm. 2024; 28(4): 1010-1021.

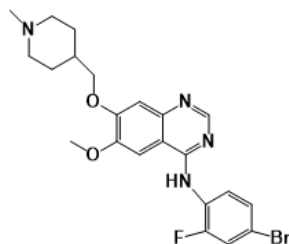


Figure 1. Chemical structure of VAN

In the literature review, various analytical methods have been reported for the determination of VAN. These include high-performance liquid chromatography (HPLC), liquid chromatography-tandem mass spectrometry (LC-MS/MS), and UV spectrophotometry [10-19]. However, as known, these conventional techniques are often associated with high costs, lengthy analysis times, and reliance on specialized equipment, such as liquid chromatography-mass spectrometers (LC-MS/MS), which may not be readily accessible in standard laboratory settings. The main goal of this study is to develop a novel, cost-effective, selective, and rapid voltammetric method for the analysis of VAN. This method aims to address the limitations of traditional analytical techniques by providing a practical alternative that can be readily employed in standard laboratory setups. However, the effectiveness of solid electrode voltammetry largely depends on the properties of the working electrode. Solid electrodes have highly active surfaces, making them particularly valuable in biological applications because they facilitate oxidation reactions and help elucidate reaction mechanisms for numerous physiologically relevant substances.

Carbon paste electrodes (CPEs) have garnered increasing attention in the field of electrochemistry, largely owing to their advantageous characteristics such as low residual currents, reduced noise levels, cost-effectiveness, ease of preparation, and replaceability. These electrodes boast a wide range of applications, encompassing both anodic and cathodic processes. Within the realm of conductive electrodes, CPEs emerge as especially promising due to their ease of modification, straightforward surface renewability, minimal background currents, and versatility in accommodating diverse analytes [20-25].

Surfactants play a pivotal role in chemistry and exert significant influence on various electrochemical processes. Their distinct amphiphilic structure and surface activity make them indispensable in electrochemical research. It is well-documented that the modification of electrode surfaces with surfactants enhances the rate of electron transfer between the electrode surface and the analyte, consequently leading to improvements in detection limits [26-33].

In the existing literature, there have been no prior reports regarding the electrochemical determination of VAN. This study marks the first instance of such determination utilizing a CPE, both in the absence and presence of surfactants. Furthermore, the developed SW-AdSV technique based on the CPE demonstrates exceptional sensitivity and selectivity for the precise determination of VAN in model serum samples.

2. RESULTS AND DISCUSSION

2.1. Detailed electrochemical behavior of VAN

The research primarily focuses on examining the current responses obtained via cyclic voltammetry of VAN on a CP electrode in aqueous media over a wide potential range. To elucidate the electrochemical behavior of VAN on the CP electrode, three consecutive CVs of a 2×10^{-5} M VAN solution were recorded at a scan rate of 100 mV s^{-1} within the potential range of 0.0 to +1.5 V (vs. Ag/AgCl) in a 0.1 M HNO_3 solution (Figure 2A). Upon examining the cyclic voltammogram, it was observed that VAN exhibited an anodic oxidation peak at approximately +1.20 V with a current of 1.45 μA . However, as the scan rate increased, particularly at 400 mV s^{-1} and subsequent rates ($v > 400 \text{ mV s}^{-1}$), reduction peaks were discerned in the cathodic region at approximately 0.44, 0.68, and 0.84 V (Figure 2B). Valuable insights into the electrode reaction mechanism (rate-determining step) can be gleaned from the relationship between peak current and scan rate. The effect of scan rate on the electrochemical oxidation of 2×10^{-5} M VAN was examined using different scan rates (5-800 mV/s) with a CP electrode in 0.1 M HNO_3 solution, and the corresponding voltammograms are depicted in Figure 2B.

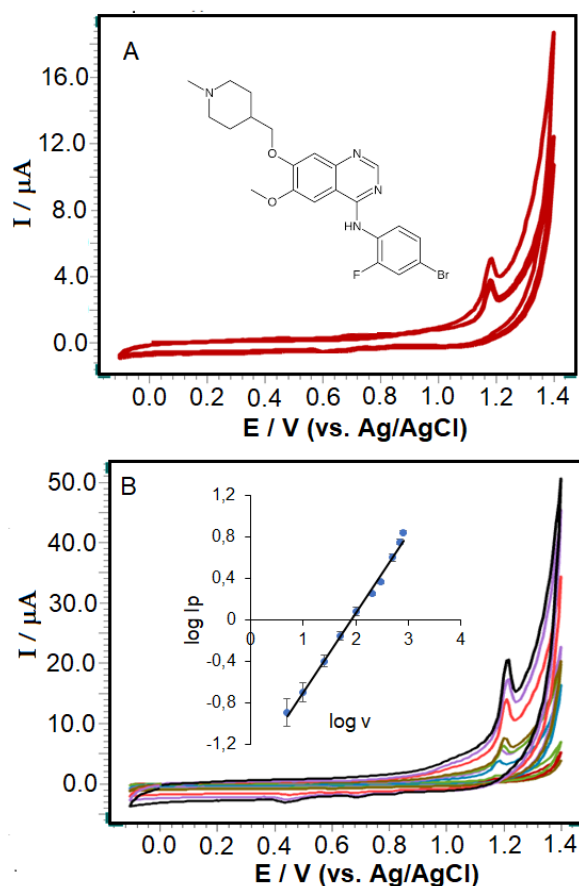


Figure 2. A- CVs of 2.0×10^{-5} M VAN at CP electrode with three repetitions in 0.1 M HNO_3 solution. The scan rate is 100 mV/s. B- CVs of 2.0×10^{-5} M VAN at different scan rates (5, 10, 25, 50, 100, 200, 300, 500, 700, and 800 mV s^{-1}) at the CP electrode. Inset: the plot of $\log i_p$ vs. $\log v$.

Graphs were plotted using the data obtained from the voltammograms, based on equations (Eq.1) and (Eq.2). The equations describing the linearity of these graphs are presented below:

For Equation (Eq.1):

$$I_p (\mu\text{A}) = 0.1272 \sqrt{v} (\text{mV/s}) - 0.3561; r = 0.9968 \quad (\text{Eq.1})$$

For Equation (Eq.2):

$$\log I_p = 0.7702 \log v - 1.4666; r = 0.9975 \quad (\text{Eq.2})$$

The observed shift of oxidation peaks towards higher potentials in CV indicates an increase in the reaction rate at the electrode surface. This suggests that all active species on the electrode surface are rapidly replenished. This slight shift arises due to the acceleration of the electrochemical reaction, and it is directly associated with the scan rate. This phenomenon serves as an important indicator for understanding the reaction kinetics and mechanism at the electrode surface. Additionally, the linear relationship between the logarithm of the oxidation peak current and the logarithm of the scan rate, as expressed by Eq. 2. above, holds true. The slope of this equation, theoretically known to be greater than 0.5, implies that the electro-oxidation of VAN is controlled by adsorption. The relationship between the oxidation peak potential and the scan rate provides valuable insights, particularly regarding the electrode reaction mechanism of VAN. Based on this information, Eq 3. relating E_p and $\log v$ is provided below.

$$E_p (\text{V}) = 0.0513 \log v + 1.1004, (r=0.9985) \quad (3)$$

According to the Laviron equation, which expresses the relationship between the potential (E_p) and the current (i) in irreversible electrochemical reactions (as Equation 4), the number of electrons involved (n) in the reaction has been calculated [34].

$$E_p = E^0 + \left(\frac{2.303RT}{\alpha nF} \right) \cdot \log \left(\frac{RTk_0}{\alpha nF} \right) + \left(\frac{2.303RT}{\alpha nF} \right) \cdot \log v \quad (4)$$

Wherein, T represents the absolute temperature, R denotes the universal gas constant, F signifies the Faraday constant, E^0 represents the formal redox potential, v indicates the scan rate, n represents the number of electrons transferred, k_0 signifies the heterogeneous transfer constant of the reaction, and α denotes the electronic transfer coefficient. Substituting the given values into the expression $E_p = (2.303RT/\alpha nF) \cdot \log v$ and considering the slope of the plot of E_p (V) versus $\log v$ (mV s^{-1}), the derived value for αn was found to be 1.1. Typically, α equals 0.5 in electrochemical irreversible reactions. Hence, $n = 2.2$ (~ 2) is obtained for the oxidation of VAN. To enhance the sensitivity and selectivity of the voltammetric determination of VAN, sharper and well-defined peaks were achieved using the SW-AdSV technique. The impact of supporting electrolyte solutions across a pH range on the electrochemical response of VAN was examined. Figure 3A illustrates SWVs of 2.0×10^{-6} M VAN across a pH range of 2.0 to 10.0 in BR buffer, with a potential range from 0.0 V to +1.4 V. Figure 3B displays SW-AdSVs of 2.0×10^{-6} M VAN conducted in 0.1 M HNO_3 , 0.1 M H_2SO_4 , and 0.1 M HClO_4 solutions, while Figure 3C exhibits SW-AdSVs in pH 2.5 and pH 7.4 phosphate buffer at the CP electrode. The oxidation peak current values recorded across these mediums are collectively presented in Figure 4.

As depicted in Figure 3A, variations in oxidation peak current and peak potential with increasing pH suggest a pH-dependent nature of the electrochemical oxidation of VAN. Examination of the oxidation peak behavior of VAN across pH 2.0 to pH 10.0 in BR buffer revealed a single sharp peak only at pH 2 and 3. At pH 4.0 and pH 5.0, the oxidation peak splits into two, accompanied by a decrease in peak current intensity. These two oxidation steps amalgamate, leading to an intensified peak at pH 6.0 and pH 7.0.

In Figure 3B-C, the electrochemical behavior of VAN in different supporting electrolytes is illustrated. Consequently, the highest anodic peak current was observed in the 0.1 M HNO_3 solution, prompting further electroanalytical studies to be conducted using this medium. Additionally, the variation of oxidation peak potential (E_p) versus pH was examined (Figure 3A, inset). A discernible potential shift towards less positive values with increasing pH indicates the pH-dependent nature of VAN oxidation. It was demonstrated by the following Eq 5. that this dependency exhibited linearity for the oxidation peaks within the pH range of 2-7.

$$E_p (\text{V}) = -0.069 \text{ pH} + 1.3059 \quad (r = 0.996) \quad (5)$$

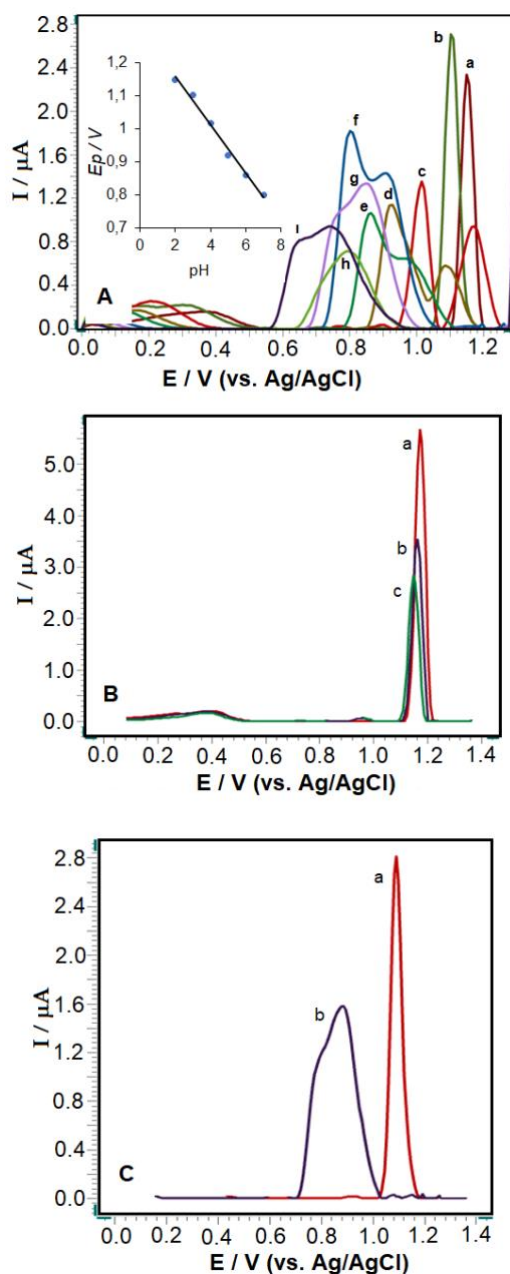


Figure 3. SW-AdSVs of 2.0×10^{-6} M VAN were conducted under various conditions: **A-** In BR buffer ranging from pH 2.0 to 10.0 (a: pH 2.0, b: pH 3.0, c: pH 4.0, d: pH 5.0, e: pH 6.0, f: pH 7.0, g: pH 8.0, h: pH 9.0, and i: pH 10.0) **B-** In different acidic solutions (a: 0.1 M HNO_3 , b: 0.1 M H_2SO_4 , c: 0.1 M $HClO_4$) **C-** In phosphate buffer at different pH values (a: pH 2.5 and b: pH 7.4). Inset: The graph (3A) illustrates E_p vs pH. SWV parameters: $\Delta E_s = 8$ mV; $f = 50$ Hz; $\Delta E_{sw} = 30$ mV. Electrochemical deposition time: 30 s (open circuit, 400 rpm).

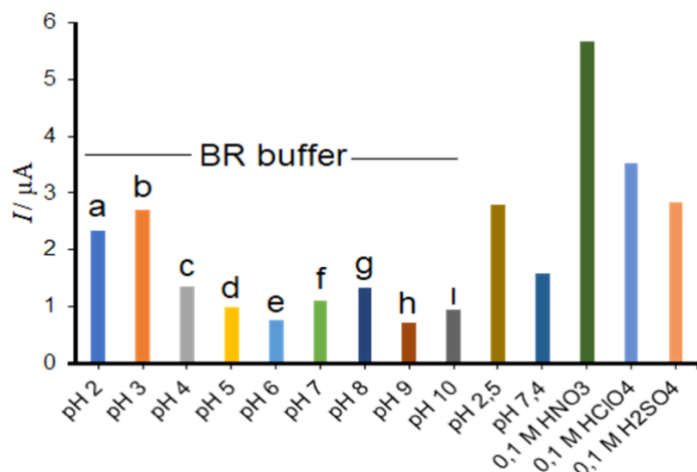
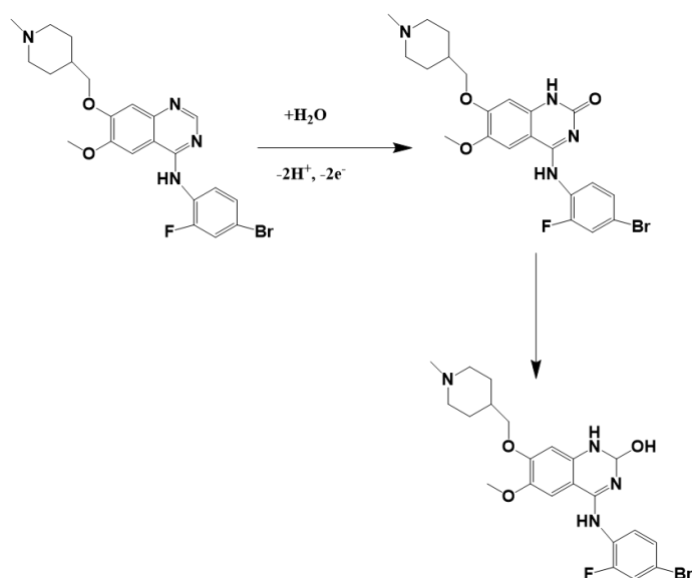


Figure 4. The oxidation peak currents of 2.0×10^{-6} M VAN in all pHs by SW-AdSV.

The linearity observed for the oxidation peak of VAN within the pH range of 2.0 to 7.0 yielded a negative slope of 69.0 mV/pH for the CP electrode. The proximity of this slope value to the theoretical value of 59 mV/pH suggests that the number of protons and electrons involved is equal in the oxidation reaction mechanism of VAN in an aqueous solution [35]. Aligned with the preceding information, it can be posited that the electrochemical oxidation of VAN predominantly takes place at the 4-amino group positioned on the quinazoline ring, constituting the primary moiety of the molecule. Synthesizing these findings, the conceivable oxidation mechanism of VAN is elucidated in Scheme 1.



Scheme 1. Proposed reaction mechanism for electro-oxidation of VAN.

In the subsequent investigation, pulse parameters including step potential ($\Delta E_s = 2\text{--}18$ mV), frequency ($f = 5\text{--}150$ Hz), and square-wave amplitude ($\Delta E_{sw} = 10\text{--}50$ mV) were meticulously adjusted to establish the optimal experimental configuration. This process entailed modifying one parameter while holding the other two constants, to enhance sensitivity in detecting the oxidation peak. The values yielding the highest sensitivity were identified as follows: $\Delta E_s = 16$ mV; $f = 75$ Hz; and $\Delta E_{sw} = 40$ mV. Furthermore, the effects of deposition time and deposition potential on the peak current of 5.0×10^{-7} M VAN were investigated under optimum experimental conditions. SW-AdSVs were recorded for this purpose. The optimal values were determined by varying the accumulation potentials in the range of (0.00) – (+1.00 V)

and the accumulation times in the range of 0.0-120.0 s. The optimum accumulation potential was found to be open circuit, and the optimal accumulation time was 30 s.

Finally, the effect of the anionic surfactant SDS (sodium dodecyl sulfate) on the electrochemical oxidation signal of VAN was evaluated. For this purpose, VAN concentration was fixed at 5.0×10^{-7} M, and SDS was added to a 0.1 M HNO_3 solution in the range of 4×10^{-4} to 1×10^{-3} M. As shown in Figure 5, a significant signal enhancement was observed in the presence of SDS. Therefore, all experiments for the remaining analytical investigation fixed the concentration of SDS at 9×10^{-4} M. In this case, the signal of VAN increased almost 12-fold compared to the surfactant-free solution.

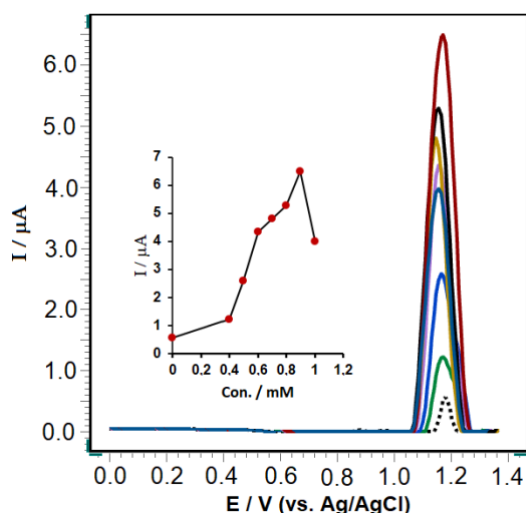


Figure 5. SW-AdSVs of 5.0×10^{-7} M VAN in 0.1 M HNO_3 in the presence of different SDS concentrations (4.0×10^{-4} – 1×10^{-3} M) are depicted. The dashed line represents the voltammograms without SDS. Inset: a plot of peak current (i_p) versus the concentration of SDS. The pre-concentration period was set at 30 s under open-circuit conditions. SWV parameters: $\Delta E_s = 16$ mV; $f = 75$ Hz; $\Delta E_{sw} = 40$ mV.

2.2. Quantification of VAN

Following all optimization experiments, parameters such as precision, accuracy, sensitivity, and selectivity were evaluated for VAN validation. The SW-AdSV technique, recognized as the most sensitive among the voltammetric techniques, was employed to record SW-AdSVs of VAN at increasing concentrations in 0.1 M HNO_3 . The relevant curves within the obtained linearity range are depicted in Figure 6, while the values for validation parameters are summarized in Table 1. Limits of quantification (LOQ) and detection (LOD) were determined by calculating ten and three times the standard deviation of the peak currents (from ten runs) of the lowest concentration (1.05×10^{-7} M) within the specified linearity range, respectively. These values were then divided by the slope of the respective calibration curves. The formulae used were $LOD = \frac{3s}{m}$ and $LOQ = \frac{10s}{m}$ respectively, where s is the standard deviation and m is the slope.

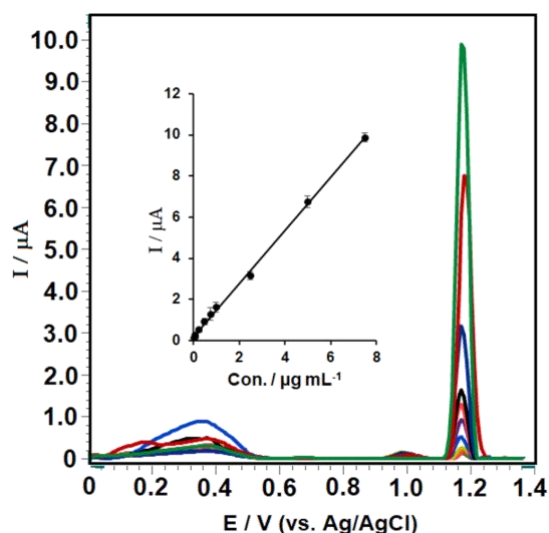


Figure 6. SW-AdSVs for VAN levels of (1–10) 1.05×10^{-7} , 1.6×10^{-7} , 2.1×10^{-7} , 5.3×10^{-7} , 1.05×10^{-6} , 1.6×10^{-6} , 2.1×10^{-6} , 5.3×10^{-6} , 1.05×10^{-5} , and 1.6×10^{-5} M in 0.1 M HNO_3 . The inset shows the corresponding calibration plot for the quantitation of VAN. The pre-concentration period was set at 30 s under open-circuit conditions. SWV parameters: $\Delta E_s = 16$ mV; $f = 75$ Hz; $\Delta E_{sw} = 40$ mV.

Table 1. Analytical parameters obtained for the oxidation peak of VAN

Analytical parameter		Oxidation peak of VAN
E_p (V)		+1.17
Linearity range, M		$1.05 \times 10^{-7} - 1.6 \times 10^{-5}$
Linear regression equation		$i_p (\mu\text{A}) = 617292 C (\text{M}) + 0.1644$
Correlation coefficient		0.9991
LOQ, M		9.0×10^{-8}
LOD, M		2.7×10^{-8}
Intra-day repeatability (RSD%, $n = 10$)	2.89 (peak current)	
	0.42 (peak potential)	
Inter-day repeatability (RSD%, $n = 5$)	3.56 (peak current)	
	0.58 (peak potential)	

This report constitutes the first comprehensive study of VAN's detection through electrochemical and analytical methods. The simplicity of the current methodology renders it applicable with sufficient analytical precision for commercial product assessment. To evaluate the precision of the proposed method, intra-day repeatability (ten experiments within the same day) and inter-day repeatability (five experiments conducted over five consecutive days by measuring the stripping responses of the same concentration of freshly prepared VAN) were calculated for 1.05×10^{-7} M of VAN under the specified experimental conditions (refer to Table 1).

In the selectivity study, no change in the peak potential of VAN was observed in the presence of inorganic compounds such as Ca^{2+} , Na^+ , K^+ , NO_3^- , Cl^- as well as biocompounds such as uric acid (UA), ascorbic acid (AA), and dopamine (DP). The oxidation potential of VAN was observed at approximately +1.17 V, while the oxidation of uric acid was observed at approximately +0.72 V. The peak potential of dopamine was approximately +0.6 V, and that of ascorbic acid was approximately +0.76 V (Figure 7). These results indicate that the method designed with the CP electrode in the presence of SDS is selective.

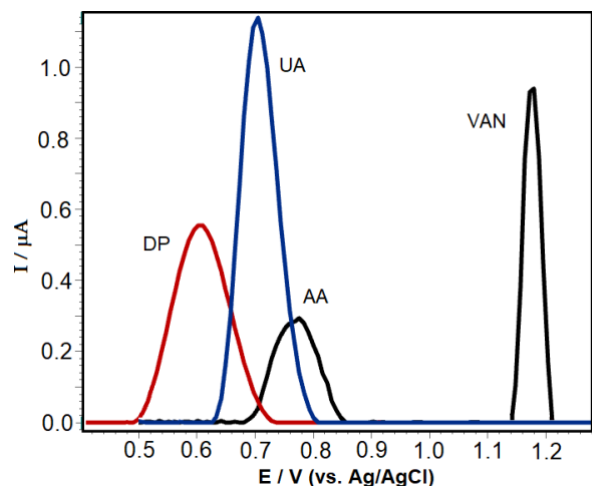


Figure 7. SW-AdSVs for 2.0×10^{-6} M DP, 4.0×10^{-6} M AA, 2.0×10^{-6} M UA and 1.0×10^{-6} M VAN in 0.1 M HNO_3 . The pre-concentration period was set at 30 s under open-circuit conditions. SWV parameters: $\Delta E_s = 16$ mV; $f = 75$ Hz; $\Delta E_{sw} = 40$ mV.

In the subsequent phase, the quantity of VAN was determined utilizing the CP electrode in the presence of 9×10^{-4} M SDS and employing the standard addition method with human serum samples. The SW-AdSV signals for the analysis of serum samples are depicted in Fig. 8. As known, the analysis of drugs extracted from biological samples typically entails significant time consumption and the utilization of costly organic solvents. However, with this technique, no pretreatment beyond the precipitation of serum proteins with acetonitrile and subsequent dilution with the chosen supporting electrolyte is required. Recovery results of VAN from serum solutions were calculated based on the respective linear regression equation (i_p (μA) = $818442 C$ (M) + 0.3937, $r: 0.998$) illustrated in Table 2. As illustrated in Fig. 8, no extraneous substance or additional noise signals from the serum samples were observed within the potential range where the oxidation peak manifested.

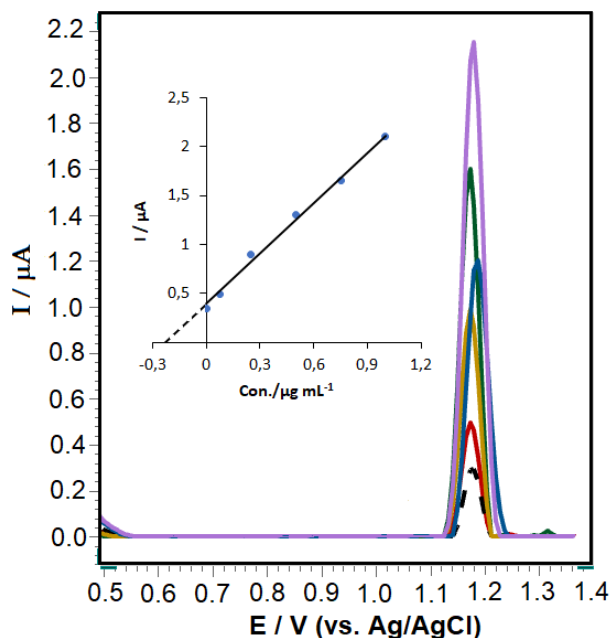


Figure 8. SW-AdSVs for human serum sample spiked VAN (---), and after standard addition of VAN 1.6×10^{-7} , 5.3×10^{-7} , 1.0×10^{-6} , 1.6×10^{-6} , and 2.0×10^{-6} in 0.1 M HNO_3 . The pre-concentration period was set at 30 s under open-circuit conditions. SWV parameters: $\Delta E_s = 16$ mV; $f = 75$ Hz; $\Delta E_{sw} = 40$ mV.

Table 2. Measurement results for addition and recovery of VAN from the serum sample

Medium	0.1 M HNO ₃
Added (µM)	1.05
Found (µM)	1.09
Number of experiments	3.0
Average recovered (%)	103.8
%RSD of recovery	1.16

3. CONCLUSION

The voltammetric analysis conducted with a carbon paste electrode in the presence of sodium dodecyl sulfate (SDS) environment yields promising results for the determination of a targeted drug, vandetanib (VAN). The analysis performed with the CP electrode in the presence of SDS demonstrates high selectivity and sensitivity for the determination of VAN. Selectivity studies reveal no significant change in the peak potential of VAN in the presence of inorganic and biological compounds. The oxidation peak potential of VAN is observed at approximately +1.17 V, while the oxidation peak potentials of various biological compounds significantly differ from this value. The linear working range was established as 1.05×10^{-7} – 1.6×10^{-5} M, with calculated LOD and LOQ values of 9.0×10^{-8} and 2.7×10^{-8} M, respectively. The method designed based on CP electrode in presence SDS proved effective in determining VAN in human serum samples. The obtained average recovery values were found to be 103.8%, when applied to spiked serum samples. Furthermore, proposing the electrochemical oxidation mechanism of VAN for the first time will assist in elucidating similar molecular structures.

4. MATERIALS AND METHODS

VAN standard pharmaceutical active ingredient was purchased from ChemScene (Türkiye, CAS. No.: 443913-73-3; Purity: 99.95%). 0.1 M Acetate buffer, ABS (4.7), 0.1 M phosphate buffer, PBS (pH 2.5, 7.4), 0.1 M Britton-Robinson buffer, BRT (pH 2.0 – 9.0), and 0.2 M H₂SO₄ (96%, Merck) were used as supporting electrolytes. Additionally, dopamine, ascorbic acid, uric acid, lactose, glucose, potassium chloride, magnesium chloride, sodium sulfate, and potassium nitrate were obtained from Sigma-Aldrich to perform interference studies. The chemicals H₃PO₄ (85%), NaH₂PO₄ · H₂O, CH₃COOH (100%), HCl (37%), H₃BO₃ (99.5%), and Na₂HPO₄ used in the preparation of supporting electrolyte solutions were obtained from Sigma-Aldrich. Electrochemical studies were carried out with cyclic voltammetry (CV), and square wave voltammetry (SWV) techniques using Autolab PGSTAT 101 (Metrohm Autolab B.V., Netherlands) electrochemical analyzer with NOVA 2.1.7 electrochemical software. Electrochemical studies were carried out using a triple electrochemical cell system containing a working electrode, counter electrode, and reference electrode. The carbon paste electrode as the working electrode (BASi, MF-2010, USA); the platinum wire (MW-1032, USA) obtained from BASi was used as the counter electrode and Ag/AgCl electrode (3 M NaCl; BASi, MF 2056, USA) was used as the reference electrode. In addition, solid chemical substances were weighed with a Vibra brand electronic scale with a sensitivity of 0.01 mg. ISOLAB model ultrasonic bath was used to clean the working electrode and dissolve some substances. WTW inoLab pH7110 digital pH meter was used to adjust the pH of the solutions. Carbon paste was prepared by homogeneously mixing 70% (w/w) graphite powder and 30% (w/w) mineral oil and pressed into the electrode. The electrode surface was turned into a homogeneous surface with wax paper. The surface of the electrode was renewed before each experiment. A certain amount of VAN and 1.0 ml of acetonitrile as a precipitating agent were added to human blood plasma samples. The solution was then transferred to centrifuge tubes and made up to a volume with 0.1 M HNO₃. Precipitated proteins were centrifuged at 5000 rpm for 10.0 min to separate the precipitate. To prepare the urine sample, membrane filters were first used and a certain amount of VAN solution was added to the urine solution. Finally, an application was made on real examples with the standard addition method.

Acknowledgements: This study was conducted with financial support from the Van Yüzüncü Yıl University Scientific Research Foundation (Project number: TSA-2022-9961). **Author contributions:** Concept – C.M., P.T.P., Z.Ş.; Design – C.M., P.T.P., Z.Ş.; Supervision – P.T.P.; Resources – C.M., P.T.P., Z.Ş.; Materials – C.M., P.T.P., Z.Ş.; Data Collection and/or Processing – C.M., P.T.P., Z.Ş.; Analyzes and/or Interpretation – C.M., P.T.P., Z.Ş.; Literature

Search – C.M., P.T.P., Z.S.; Writing – C.M., P.T.P., Z.S.; Critical Reviews – C.M., P.T.P., Z.S.;

Conflict of interest statement: The authors declared no conflict of interest.

REFERENCES

- [1] La Salvia A, Espinosa-Olarte P, Riesco-Martinez MDC, Anton-Pascual B, Garcia-Carbonero R. Targeted cancer therapy: what's new in the field of neuroendocrine neoplasms?. *Cancers*. 2021; 13(7): 1701. <https://doi.org/10.3390/cancers13071701>.
- [2] Shyam Sunder S, Sharma UC, Pokharel S. Adverse effects of tyrosine kinase inhibitors in cancer therapy: pathophysiology, mechanisms and clinical management. *Signal Transduct Target Ther*. 2023; 8(1): 262. <https://doi.org/10.1038/s41392-023-01469-6>
- [3] Anand U, Dey A, Chandel AKS, Sanyal R, Mishra A, Pandey DK, Pérez de la Lastra JM. Cancer chemotherapy and beyond: Current status, drug candidates, associated risks and progress in targeted therapeutics. *Genes Dis*. 2023; 10(4): 1367–1401. <https://doi.org/10.1016/j.gendis.2022.02.007>.
- [4] Thornton K, Kim G, Maher VE, Chattopadhyay S, Tang S, Moon YJ, Pazdur R. Vandetanib for the treatment of symptomatic or progressive medullary thyroid cancer in patients with unresectable locally advanced or metastatic disease: US Food and Drug Administration drug approval summary. *Clin Cancer Res*. 2012; 18(14): 3722–3730. <https://doi.org/10.1158/1078-0432.CCR-12-0411>
- [5] Durante C, Paciaroni A, Plasmati K, Trulli F, Filetti S. Vandetanib: opening a new treatment practice in advanced medullary thyroid carcinoma. *Endocrine*. 2013; 44: 334–342. <https://doi.org/10.1007/s12020-013-9943-9>
- [6] Trimboli P, Castellana M, Virili C, Giorgino F, Giovannella L. Efficacy of vandetanib in treating locally advanced or metastatic medullary thyroid carcinoma according to RECIST criteria: a systematic review and meta-analysis. *Front Endocrinol*. 2018; 9: 224. <https://doi.org/10.3389/fendo.2018.00224>
- [7] Tsang VH, Robinson BG, Learoyd DL. The safety of vandetanib for the treatment of thyroid cancer. *Expert Opin Drug Saf*. 2016; 15(8): 1107–1113. <https://doi.org/10.1080/14740338.2016.1201060>
- [8] Dall'Acqua S, Vedaldi D, Salvador A. Isolation and structure elucidation of the main UV-A photoproducts of vandetanib. *J Pharm Biomed Anal*. 2013; 84: 196–200. <https://doi.org/10.1016/j.jpba.2013.05.049>
- [9] Maluleka MM, Mokoena TP, Mampa RM. Synthesis, crystal, and Hirschfeld surface, DFT and molecular docking studies of 6-(3-chloro-4-fluorophenyl)-4-ethoxy-2-(4-methoxyphenyl) quinazoline derivative. *J Mol Struct*. 2022; 1255: 132439. <https://doi.org/10.1016/j.molstruc.2022.132439>
- [10] Lin H, Cui D, Cao Z, Bu Q, Xu Y, Zhao Y. Validation of a high-performance liquid chromatographic ultraviolet detection method for the quantification of vandetanib in rat plasma and its application to pharmacokinetic studies. *J Cancer Res Cell Ther*. 2014; 10(1): 84–88. <https://doi.org/10.4103/0973-1482.131393>
- [11] Alanazi MM, Obaidullah AJ, Attwa MW. A Novel Green Micellar HPLC-UV method for the estimation of vandetanib in pure form, human urine, human plasma and human liver microsomes matrices with application to metabolic stability evaluation. *Molecules*. 2022; 27(24): 9038. <https://doi.org/10.3390/molecules27249038>
- [12] Darwish HW, Bakheit AH, Al-Shakliah NS, Darwish, IA. Development of novel response surface methodology-assisted micellar enhanced synchronous spectrofluorimetric method for determination of vandetanib in tablets, human plasma and urine. *Spectrochim Acta A Mol Biomol Spectrosc*. 2019; 213: 272–280. <https://doi.org/10.1016/j.saa.2019.01.056>
- [13] Attwa MW, Kadi AA, Darwish HW, Amer SM, Al-Shakliah NS. Identification and characterization of in vivo, in vitro and reactive metabolites of vandetanib using LC-ESI-MS/MS. *Chem Cent J*. 2018; 12: 1–16. <https://doi.org/10.1186/s13065-018-0467-5>
- [14] Merienne C, Rousset M, Ducint D, Castaing N, Titier K, Molimard M, Bouchet S. High throughput routine determination of 17 tyrosine kinase inhibitors by LC-MS/MS. *J Pharm Biomed Anal*. 2018; 150: 112–120. <https://doi.org/10.1016/j.jpba.2017.11.060>
- [15] Bai F, Johnson J, Wang F, Yang L, Broniscer A, Stewart CF. Determination of vandetanib in human plasma and cerebrospinal fluid by liquid chromatography electrospray ionization tandem mass spectrometry (LC-ESI-MS/MS). *J Chromatogr B*. 2011; 879(25): 2561–2566. <https://doi.org/10.1016/j.jchromb.2011.07.012>
- [16] Salode VL, Game MD, Salode GV, Gadge SS. Development of validated stability indicating method for estimation of Vandetanib and characterization of its degradants by LC-ESI-MS. *Indian J Pharm Educ Res*. 2022; 56(1): 232–239.
- [17] Khandare B, Dudhe PB, Upasani S, Dhoke M. Spectrophotometric determination of vandetanib in bulk by area under curve and first order derivative methods. *nt J Pharmtech Res*. 2019; 12: 103–110. <https://doi.org/10.20902/IJPTR.2019.120202>
- [18] Dall'Acqua S, Vedaldi D, Salvador A. Isolation and structure elucidation of the main UV-A photoproducts of vandetanib. *J Pharm Biomed Anal*. 2013; 84: 196–200. <https://doi.org/10.1016/j.jpba.2013.05.049>
- [19] Abdelhameed AS, Hassan ES, Attwa MW, Al-Shakliah NS, Alanazi AM, AlRabiah H. Simple and efficient spectroscopic-based univariate sequential methods for simultaneous quantitative analysis of vandetanib, dasatinib, and sorafenib in pharmaceutical preparations and biological fluids. *Spectrochim Acta A Mol Biomol Spectrosc*. 2021; 260: 119987. <https://doi.org/10.1016/j.saa.2021.119987>

- [20] Aydin I, Akgun H, Talay Pinar P. Analytical determination of the oxazolidinone antibiotic linezolid at a pencil graphite and carbon paste electrodes. *ChemistrySelect*. 2019; 4(34): 9966-9971. <https://doi.org/10.1002/slct.201902269>
- [21] Göktaş D, Talay Pinar P. First report for the electrochemical determination and proposed mechanism of poly (ADP ribose) polymerase inhibitor and new smart anticancer drug olaparib. *Monatsh Chem*. 2023; 154(6): 577-584. <https://doi.org/10.1007/s00706-023-03069-0>
- [22] Monnappa AB, Manjunatha JG, Bhatt AS. Design of a sensitive and selective voltammetric sensor based on a cationic surfactant-modified carbon paste electrode for the determination of alloxan. *ACS Omega*. 2020; 5(36): 23481-23490. <https://doi.org/10.1021/acsomega.0c03517>
- [23] Vural K, Karakaya S, Dilgin DG, Gökçel Hİ. Dilgin Y. Voltammetric determination of Molnupiravir used in treatment of the COVID-19 at magnetite nanoparticle modified carbon paste electrode. *Microchem J*. 2023; 184: 108195. <https://doi.org/10.1016/j.microc.2022.108195>
- [24] Turunc E, Gumus I, Arslan H. Redox active Co (II) complex modified carbon paste electrode for the determination of dopamine. *Mater Chem Phys*. 2020; 243: 122597. <https://doi.org/10.1016/j.matchemphys.2019.122597>
- [25] Aydoğmuş Z, Aslan SS, Yildiz G, Senocak A. Differential pulse voltammetric determination of anticancer drug regorafenib at a carbon paste electrode: electrochemical study and density functional theory computations. *J Anal Chem*. 2020; 75: 691-700. <https://doi.org/10.1134/S1061934820050032>
- [26] Housaindokht MR, Janati-Fard F, Ashraf N. Recent advances in applications of surfactant-based voltammetric sensors. *J Surfactants Deterg*. 2021; 24(6): 873-895. <https://doi.org/10.1002/jsde.12541>
- [27] Talay Pinar P. Electrooxidation and low-tech determination of pantoprazole on a disposable pencil graphite electrode by the use of cationic surfactant. *Acta Chim Slov*. 2020; 67(1): 212-220. <https://doi.org/10.17344/acsi.2019.5367>
- [28] Ziyatdinova G, Yakupova E, Davletshin R. Voltammetric determination of hesperidin on the electrode modified with SnO₂ nanoparticles and surfactants. *Electroanalysis*. 2021; 33(12): 2417-2427. <https://doi.org/10.1002/elan.202100405>
- [29] Sener CE, Dogan Topal B, Ozkan SA. Effect of monomer structure of anionic surfactant on voltammetric signals of an anticancer drug: rapid, simple, and sensitive electroanalysis of nilotinib in biological samples. *Anal Bioanal Chem*. 2020; 412: 8073-8081. <https://doi.org/10.1007/s00216-020-02934-9>
- [30] Tigari G, Manjunatha JG. A surfactant enhanced novel pencil graphite and carbon nanotube composite paste material as an effective electrochemical sensor for determination of riboflavin. *J Sci Adv Mater Devices*. 2020; 5(1): 56-64. <https://doi.org/10.1016/j.jsamd.2019.11.001>
- [31] Altunkaynak Y, Önal G, Levent A. Application of boron-doped diamond electrode for rapid and sensitive voltammetric detection of vildagliptin in anionic surfactant medium. *Monats Chem*. 2023; 154(2): 181-190. <https://doi.org/10.1007/s00706-022-03020-9>
- [32] Önal G, Altunkaynak Y, Levent A. Application of BiFE for electrochemical properties and determination of loratadine by cathodic stripping voltammetry in the cationic surfactant medium. *J Iran Chem Soci*. 2021; 18(12): 3465-3475. <https://doi.org/10.1007/s13738-021-02286-w>
- [33] Altunkaynak Y, Önal G, Levent A. Electrochemical evaluation of the desloratadine at bismuth film electrode in the presence of cationic surfactant: Highly sensitive determination in pharmaceuticals and human urine by Linear sweep-cathodic stripping voltammetry. *Turk J Chem*. 2021; 45(3): 775-787. <https://doi.org/10.3906/kim-2101-42>
- [34] Laviron EJJ. General expression of the linear potential sweep voltammogram in the case of diffusionless electrochemical systems. *J Electroanal Chem Interfacial Electrochem*. 1979; 101(1): 19-28. [https://doi.org/10.1016/S0022-0728\(79\)80075-3](https://doi.org/10.1016/S0022-0728(79)80075-3)
- [35] Bakirhan NK, Tok TT, Ozkan SA. The redox mechanism investigation of non-small cell lung cancer drug: Erlotinib via theoretical and experimental techniques and its host-guest detection by β -Cyclodextrin nanoparticles modified glassy carbon electrode. *Sens Actuators B*. 2019; 278: 172-180. <https://doi.org/10.1016/j.snb.2018.09.090>